(Micro-)Plastics in Saturated and Unsaturated Groundwater Bodies: First Evidence of Presence in Groundwater Fauna and Habitats

sustainability

MDPI

Article

(Micro-)Plastics in Saturated and Unsaturated Groundwater Bodies: First Evidence of Presence in Groundwater Fauna and Habitats

Laura Sforzi [1], Agostina Tabilio Di Camillo [2,3,*], Tiziana Di Lorenzo [3,4,5,6], Diana Maria Paola Galassi [2], Valentina Balestra [7,8,9], Leonardo Piccini [10], Serena Benedetta Cabigliera [1], Samuele Ciattini [11], Marco Laurati [1,12], David Chelazzi [1,12], Tania Martellini [1,12] and Alessandra Cincinelli [1,12]

1 Department of Chemistry "Ugo Schiff", University of Florence, Via della Lastruccia, 3-13, 50019 Sesto Fiorentino, Italy; laura.sforzi@unifi.it (L.S.); serenabenedetta.cabigliera@unifi.it (S.B.C.); marco.laurati@unifi.it (M.L.); david.chelazzi@unifi.it (D.C.); tania.martellini@unifi.it (T.M.); alessandra.cincinelli@unifi.it (A.C.)
2 Department of Life, Health and Environmental Sciences, University of L'Aquila, Via Vetoio, 67100 L'Aquila, Italy; dianamariapaola.galassi@univaq.it
3 Research Institute on Terrestrial Ecosystems of the National Research Council of Italy (IRET CNR), 50019 Florence, Italy; tiziana.dilorenzo@cnr.it
4 NBFC (National Biodiversity Future Center), 90133 Palermo, Italy
5 "Emil Racovita" Institute of Speleology, 050711 Cluj-Napoca, Romania
6 3cE3c—Centre for Ecology, Evolution and Environmental Changes & CHANGE—Global Change and Sustainability Institute, Departamento de Biologia Animal, Faculdade de Ciências, Universidade de Lisboa, Campo Grande, 1749-016 Lisbon, Portugal
7 Department of Environment, Land and Infrastructure Engineering, Politecnico di Torino, Corso Duca degli Abruzzi 24, 10129 Torino, Italy; valentina.balestra@polito.it
8 Biologia Sotterranea Piemonte—Gruppo di Ricerca, Bossea Cave, Frabosa Soprana, 12082 Cuneo, Italy
9 Struttura Operativa Bossea CAI—Underground Karst Laboratory of Bossea Cave, Bossea Cave, Frabosa Soprana, 12082 Cuneo, Italy
10 Department of Earth Sciences, University of Florence, 50121 Florence, Italy; leonardo.piccini@unifi.it
11 Centro Interdipartimentale di Cristallografia, Università degli Studi di Firenze, Via della Lastruccia 5, 50019 Sesto Fiorentino, Italy; samuele.ciattini@unifi.it
12 Consorzio Interuniversitario per lo Sviluppo dei Sistemi a Grande Interfase (CSGI), University of Florence, Via della Lastruccia 3, 50019 Sesto Fiorentino, Italy
* Correspondence: agostina.tabiliodicamillo@iret.cnr.it

Abstract: Microplastic (MP) pollution is a growing concern in every known ecosystem. However, MP presence in groundwaters and the ecological impact they can have on groundwater fauna is still poorly investigated. Here, we assess the presence of MPs in three Italian groundwater bodies, comprising two karst caves and two monitoring bores of a saturated alluvial aquifer. In addition to water samples, groundwater invertebrates were collected to assess their potential ingestion of MPs. For water samples, chemical characterization of polymers was done by Fourier Transform Infrared Spectroscopy (FTIR) 2D imaging, while fauna samples were analyzed with a tandem microscopy approach (fluorescence microscopy and FTIR). The abundance of MPs in water samples varied from 18 to 911 items/L. The majority of MPs were fibers (91%), with a mean size in the range of 100 µm and 1 mm. Black, red, and blue were the most abundant colors (30%, 25%, and 19%, respectively). The most abundant polymer was artificial/textile cellulose (65%), followed by PET (21%). MPs were found in every groundwater taxon. Pellets were the most abundant in each specimen (87% on average), while the largest were fragments, with a mean dimension of 26 µm. Cellulose was found to be the most abundant polymer (51%). This study is the first to highlight the presence of MPs ingested by groundwater fauna. Further investigations are urgently required to assess the potential ecological impact MPs can have on the resident fauna in these sensitive ecosystems.

Keywords: plastic polymers; stygofauna; cave; alluvial aquifer; µFTIR; fluorescence microscopy

Citation: Sforzi, L.; Tabilio Di Camillo, A.; Di Lorenzo, T.; Galassi, D.M.P.; Balestra, V.; Piccini, L.; Cabigliera, S.B.; Ciattini, S.; Laurati, M.; Chelazzi, D.; et al. (Micro-)Plastics in Saturated and Unsaturated Groundwater Bodies: First Evidence of Presence in Groundwater Fauna and Habitats. *Sustainability* **2024**, *16*, 2532. https://doi.org/10.3390/su16062532

Academic Editors: Yanwei Li, Diannan Lu, Weiliang Dong and Yong Xiao

Received: 12 January 2024
Revised: 5 March 2024
Accepted: 15 March 2024
Published: 19 March 2024

1. Introduction

Plastic production has increased globally over the last decade, reaching 390.7 Mt of production in 2021, with the majority being fossil-based plastics [1]. Due to increasing global plastic consumption, poor waste management, and indiscriminate dispersal of post-consumer products, plastic ends up in the environment and accumulates there. Nowadays, plastics represent one of the major sources of pollution and no known ecosystem is immune to their presence [2]. Persistence in an open environment and exposition to weathering lead to the degradation of large plastics to form microplastics (MPs). MPs are defined as polymers with a dimension between 5 mm and 1 µm [3]. They can be found in a wide variety of shapes, colors, and compositions. They can be considered primary MPs, if intentionally produced, used mainly in personal care and cosmetic products (PPCPs) and household cleaners [4,5], or secondary MPs, if they originate from the fragmentation and degradation of large plastic pieces by chemical, physical or biological phenomena [6–8]. Currently, MP pollution has been found in aquatic, terrestrial, and even atmospheric environments, e.g., [9–12]. Due to their chemical and physical properties such as lightness, durability, and difficult biodegradability, once in the environment, MPs can easily reach remote regions [13,14], pointing out the ubiquity of this contaminant. Although most aquatic environments are heavily investigated for MP pollution, only a few studies address the MP presence in subterranean systems, such as cave waters, underground streams, and aquifers, e.g., [15–18]. Groundwaters are the largest source of freshwater on Earth, providing more than 2 billion people with clean water for cooking, farming, and industrial uses, including people living in both developing and developed countries [19]. MPs can reach these environments through various pathways, such as migration from soil through surface runoff, leaching from landfill and wastewater effluent, or atmospheric deposition [20]. Hydrogeological factors can play a fundamental role in MP transport in underground environments, as soil pores can create continuous channels that allow MPs to pass through the porous material of alluvial aquifers [20], or fissures and solution conduits in karst [21]. Given their small size, MPs are highly bioavailable and their large distribution in ecosystems makes them a potentially hazardous substance [22]. This is a matter of concern as some organisms may exchange plastics for prey or ingest them with food [23,24]. The impact of MP pollution may be related to their ability to act as carriers of flame retardants [25], bisphenol A (BPA) [26], phthalate esters [27] heavy metals [28], and even antibiotics [29]. Moreover, plasticizers, UV stabilizers, and pigments can be present in the plastics themselves and be released into the environment or transferred through the food chain, posing serious health problems [30,31].

In addition to groundwater investigations, there is also a lack of studies investigating the presence of MPs in groundwater metazoans. Subterranean ecosystems host stygofauna—named after the ancient Greek mythological underground river Styx—which includes groundwater-obligate invertebrate and vertebrate species [32]. These animals—also named stygobites—have evolved morphological (depigmentation, anophthalmia/microphthalmia, elongation of sensory organs), physiological, and behavioral adaptations to survive and thrive in permanently dark environments characterized by low oxygen concentration and scarce trophic resources [33]. They often represent phylogenetically ancient species with a point-like distribution and individuals living in small, clustered populations [34]. Groundwater communities are characterized by low abundance and alpha diversity, reduced functional diversity, and high beta diversity [35]. Therefore, these communities are poorly resilient and can be severely affected by the deterioration of their environmental conditions [36]. Groundwater animals provide valuable ecosystem services [37]. Many of them feed on viruses and bacteria, thus helping to remove pathogenic organisms from water intended for human consumption [37]. They are key players in the recycling of organic carbon in subterranean environments and, through their movement and fecal release, contribute to the remixing and spiking of sediments [38]. This activity contributes to keeping open the interstitial spaces (thereby, facilitating water passage, oxygenation of sediments, and dilution of pollutants) and spreading bacteria into environments not

yet colonized [37]. Despite existing research highlighting the impacts of MPs on aquatic benthic organisms, such as reduced feeding [37], stunted growth, and induced toxicity and oxidative stress [39], there is a notable lack of evidence regarding their effects in groundwater organisms. Even the fundamental aspect of MP ingestion by groundwater fauna remains unexplored. This knowledge gap is particularly alarming, given the critical role of groundwater fauna in organic carbon recycling within these ecosystems. If these organisms were to replace their natural diet with MPs, they could severely disrupt this essential ecosystem service, undermining the health and stability of groundwater environments.

To fill these gaps, this research aims to: (i) provide an initial understanding of MP presence in three Italian groundwater bodies (GWBs) influenced by human activities; (ii) analyze water samples; and (iii) assess the potential MP ingestion by stygobitic invertebrates residing in these GWBs, evaluating the occurrence of these pollutants in groundwater invertebrate fauna to better understand the extent of MP contamination and its implications for the depletion of ecosystem services. Addressing these knowledge gaps is not only crucial for preserving groundwater ecosystems but also aligns with the overarching goals of environmental sustainability and the protection of our planet's vital resources.

2. Materials and Methods

2.1. Study Area

The study area includes three Italian groundwater bodies, two in karst terrain (one touristic and one speleological cave), and one in alluvial deposits (Figure 1). Sampled caves develop in the vadose zone of karst, so groundwater mainly flows through fissures and dissolution conduits with a vertical pattern.

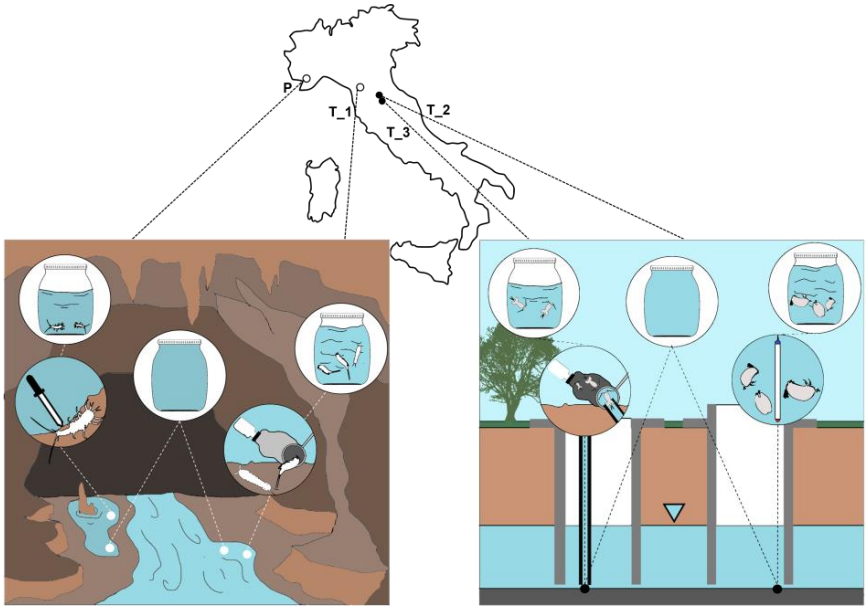

Figure 1. Map of the locations of the four sampling sites and a schematic representation of the collection methods of faunal and water samples. Left panel: sampling in the two karst caves. In detail: collection of *Proasellus franciscoloi* from Bossea Cave (P) by using a pipette (**left side**); collection of water samples in glass jars (**middle**); and collection of harpacticoids from Buca del Vasaio (T_1) by using a hand net (right side). Right panel: sampling in the two sites of the alluvial aquifer. In detail: collection of cyclopoids from bore T_2 by using a submerged pump and a net (**left side**); collection of water samples in glass jars (**middle**); collection of ostracods through bore T_3 by using a bailer (**right side**). White dots: caves; black dots: bores; light blue triangle: aquifer water table.

Bossea Cave (P; WGS84 coordinates: 44.2419285 7.8408508), the first show cave in Italy (1874), is a unique underground system located at the tectonic contact between limestone and non-soluble metavolcanic rocks, in the western Ligurian Alps, near the Maritime Alps

in Piedmont. The Bossea catchment area, which ranges from 800 to 1700 m in altitude, receives water from a combination of widespread sources consisting of external streams and small creeks originating from less permeable Permian metamorphic rocks and quartzite [40]. This catchment area covers an area of approximately 5.5 km^2. The cave itself extends for nearly 3 km and is divided into two distinct sections. An underground river, named Mora River, flows through a gorge carved into Mesozoic marble rock. Above this canyon, an intricate network of ancient epi-phreatic tunnels exists. The furthest upstream portion of the cave ends with two submerged sections, connected by a system of underground channels, with depths reaching up to 70 m below the surface. The water from the cave resurfaces at 812 m above sea level (a.s.l.) into the Corsiglia River, a significant tributary of the Tanaro River, through a group of springs. The cave entrance, situated at 836 m a.s.l., is a semi-active tunnel that discharges water during heavy floods, particularly when the springs of Bossea cannot manage the entire water flow [41]. Since 1969, inside the cave, different underground laboratories have been built to study radon activity, subterranean biology, climatology, and hydrogeology, managed by the Struttura Operativa Bossea CAI, Biologia Sotterranea Piemonte–Gruppo di Ricerca, and the Department of Environment, Land and Infrastructure Engineering (DIATI) of the Politecnico di Torino, in collaboration with ARPA Piemonte, ARPA Valle d'Aosta, and INRiM.

The Buca del Vasaio del Motrone (T_1; WGS84 coordinates: 44.0071287 10.4686116) is a cave inaccessible to the public located at the extreme south-eastern edges of the Apuan Alps in Tuscany [42]. The cave extends inside siliceous limestones with a horizontal setting. The overall length is approximately 600 m with a total height difference of about 110 m. The cave collects the infiltration waters of an overlying plateau feeding semi-dispersive water circulation. The percolation forms drips and veils of water on the walls which collect in small pools and lakes, feeding a small stream whose flow rate rarely exceeds 1 L/s.

The alluvial groundwater body, Piana alluvionale di Firenze–Prato–Pistoia, covering an area of 191 km^2 [43] in Tuscany, hosts a mixed confined–unconfined aquifer, consisting of various hydrogeological complexes with variable permeability closely related to the mean grain size of the individual litho-stratigraphical units. The substrate is composed of marly limestones, marls, sandstones, and shales. Above these low-permeable lithological units lies the entire sequence of alluvial deposits, characterized by a basal sequence of silty-clay lacustrine sediments with occasional gravel and sand layers, followed by a sequence of predominantly coarse-grained fluvial deposits. The aquifer formed by the layer of alluvial deposits houses a shallow groundwater table, which, in the Florence area, is typically found at depths ranging from 1 to 10 m. These depths may exhibit seasonal variations and are contingent upon factors such as the water supply from surface streams, the efficacy of rainfall in the region, and the occurrence of surface runoff [44]. Two sampling sites have been identified in the alluvial groundwater body. The first is a borehole utilized for irrigating a public garden in Florence (T_2; WGS84 coordinates: 43.7768304 11.1903244), and the second is a borehole employed for watering the green spaces of a research center (T_3; WGS84 coordinates: 43.8184469 11.1973391). At the sampling sites, the alluvial groundwater body is characterized by gravel (16–4 mm), sand (3–0.063 mm), and silt (<0.063 mm). Permeability is high (coefficient of permeability ranging from 1×10^{-4} to 1×10^{-2}) and effective porosity is in the range 0.09 to 0.15 [44].

2.2. Sample Collection

For the investigation of MP pollution in groundwater, it is essential to consider sampling volumes. Some authors suggest sampling at least 500–1000 L [16,45] to increase the representativeness of the samples and to better assess the concentration in this type of site, as the expected concentration of MPs is far lower than what can be found in other aquatic environments, such as surface waters [46,47]. However, this work focused on the preliminary characterization of MPs in water and fauna samples from three groundwater bodies to provide a first estimate of MP pollution and potential ecological impacts on local fauna.

Four groundwater samples along with four stygofauna pool samples were collected at each sampling site between December 2022 and March 2023. The sites were chosen to assess different levels of contamination, as two types of groundwater bodies were considered, differently exposed to anthropic factors. The most suitable sampling methods were adapted to the specificities of each sampling site (accessibility, pump availability, collectible volume), and are briefly described below. The water samples collected within the two caves, Bossea (P) and Buca del Vasaio (T_1), were collected directly as grab samples in glass jars, as the difficult accessibility of the site does not allow for the transport of bulky equipment. The alluvial aquifer (T_2, T_3) was sampled by means of groundwater monitoring bores. The composition of the hose, pumps, and coatings eventually present down the wells was noted to assess the possible release and contamination of the samples. Bore T_2, measuring 16 cm in diameter and 10 m in depth with a sealed surface, was equipped with a permanent immersion pump operating at a rate of approximately 1 L/s. Prior to sampling, we purged the entire bore column eight times and then collected 2 L of water in an amber glass bottle. This bore was encased in a pipe with perforations corresponding to the most productive aquifer layers, typically consisting of permeable gravel beds [43,44]. These layers typically comprise buried paleoconoids composed of coarse gravel, which are hydrologically fed by the hillside [43,44]. In contrast, bore T_3, with a diameter of 1 m and a depth of 6 m, remained open at the surface and was not equipped with a pump or purged. For sampling, we collected two liters of bore water using a metal bucket and stored it in an amber glass bottle. Each sample was immediately capped and sealed to prevent atmospheric contamination, then transported to the laboratory and stored refrigerated at 4 °C until analysis.

Concurrently to water samples, stygofauna pools were collected for each location. Specimens subjected to analysis all belonged to the Crustacea. Specifically, one *Proasellus franciscoloi* (Chappuis, 1955) of the Order Isopoda (Figure 2), 15 copepods of the Order Harpacticoida, 6 copepods of the Order Cyclopoida, and 19 individuals of the Class Ostracoda were examined.

Figure 2. Lateral (**left**) and ventral (**right**) perspectives of a female specimen of the isopod *Proasellus franciscoloi* (Chappuis, 1955). This species exhibits typical adaptations of the groundwater-obligated fauna, i.e., elongation of sensory appendages, depigmentation, anophthalmia, and elongated and slender body shape. The ventral side also reveals a large and rich-in-vitellum egg, a recurrent trait of the hypogean fauna.

The specimens of *P. franciscoloi* were collected at "Ramo superiore" within Bossea Cave (P site), in the speleological area through which it is possible to reach the Secondary Lab (unsaturated karst habitat). The specimens, which can easily be found on the wooden beams of the old walkway collapsed in the water, were collected with brushes, and carefully placed in glass containers, filled with groundwater, wood fragments, and sediment from the collection site. The specimens were placed in an artificial pool inside the cave, directly connected to the running water of the karst system, until they were transferred. During transportation, specimens, groundwater, wood fragments, and sediments were placed in glass containers and stored in a temperature-controlled environment. The day after collection, the specimens were transported to the laboratory, strictly following the procedures outlined in [48]. In the laboratory, deceased individuals were isolated and stored in glass vials filled with 96% ethanol.

Harpacticoida specimens were collected from the Buca del Vasaio cave (T_1 site; unsaturated karst habitat) using a 60 µm mesh net to effectively filter water, sediment, and fauna following disturbance of the substrate according to the methodology described in Malard et al. [49].

Cyclopoida specimens were sampled from the bore T_2 site (saturated alluvial habitat) from which 500 L of groundwater were extracted using the immersion pump and subsequently filtered through a 60 µm mesh net to capture the groundwater fauna, which was then transferred to a glass container [49].

Ostracoda specimens were gathered from the bore T_3 site (saturated alluvial habitat) following the method outlined in Malard et al. [49]. A sampling bailer was carefully lowered into the bore, reaching the bottom before being raised to filter the entire column of groundwater, resulting in the filling of a 2 L glass bottle. The collected fauna samples were carefully transferred to a glass container and promptly transported to the laboratory within one hour, maintaining a refrigerated environment.

Sorting and identification were carried out with a LEICA M80 stereomicroscope at 16× magnification, followed by the preservation of deceased individuals in glass vials containing 96% ethanol. A LEICA M205C stereomicroscope with an integrated camera was used to take pictures of each specimen, and LAS software (Leica Application Suite, version 4.7.1) was then used to measure body size. Conversion formulas were used to convert body size (length and width in mm) to biovolume. To convert biovolume to fresh weight, a specific gravity of 1.1 was assumed. In detail, biomasses (µg of dry mass) of the individuals of Cyclopoida, Harpacticoida, and Ostracoda were determined using the methods and size-biomass conversion equations in Reiss and Schmid-Araya's [50], while, for those of Isopoda, the conversion equation in Cummins et al. [51] was used. The harpacticoids found in T_1 consisted of the stygobitic species *Elaphoidella phreatica* (Chappuis, 1925) and the stygophile (i.e., facultative groundwater species [52]) *Bryocamptus echinatus* (Mrázek, 1893). The cyclopoids discovered in T_2 were all copepodite stages attributable to the genus *Diacyclops* Kiefer, 1927. The juvenile ontogenetic stage did not allow for the identification of individuals at the species level, leaving their ecological classification uncertain. Lastly, the ostracods found at the T_3 site could not be determined at the species level but belong to the family Candonidae. All crustacean taxa investigated in this study are deposit-feeders, i.e., ingest sediment particles and derive nutrition from organic material intermixed with these particles [53].

2.3. Microplastic Extraction

Once in the laboratory, the samples were processed as follows. Since organic and inorganic content may impair the chemical characterization, it was assessed whether pretreatment of the samples was necessary. To dissolve organic matter, samples were added at a 1:2 volume-to-volume ratio of H_2O_2 (30%, Honeywell, Offenbach am Main, Germany) sealed with aluminum foil, and left for 48 h at 60 °C [54]. Despite the oxidative treatment, some undigested inorganic matter remained at the bottom. To enhance the extraction of MPs, a saturated NaCl solution with a 1:2 volume-to-volume ratio was added to increase

water density [55]. After shaking for 1 min, the solutions were sealed with aluminum foil and allowed to settle for 24 h at room temperature. Then, the supernatant, which contained the plastic items, was filtered. The extraction was repeated three times for each sample. All samples were vacuum-filtered through a Büchner glass funnel on glass fiber filters (CHMLAB GROUP, GF3 grade, 47 mm) and dried.

The fauna samples were treated according to the methodology outlined in Di Lorenzo et al. [56]. Briefly, initially, the specimens were rinsed with ultrafiltered MilliQ water to eliminate any external particles, following ISO Standard Method SS-EN ISO 6330 [57]. Subsequently, the specimens were carefully loaded into 10 mL glass vials using a steel needle. The vials were filled with 10 mL of 30% H_2O_2 (30% SigmaAldrich, purchased from Merck, Darmstadt, Germany), sealed with aluminum foil, and maintained at a controlled temperature of 60 °C for 72 h to digest the organic matter [58]. Then, samples were vacuum-filtered through a 2 cm ceramic Büchner funnel diameter onto glass fiber filters (CHMLAB GROUP, GF3 grade) and dried. These filters could be directly subjected to spectroscopic analysis (see Section 2.5). Inspection through fluorescence microscopy required further processing using the lipophilic dye Nile Red to stain the entire filters [59]. A few drops of Nile Red dye solution in ethanol were poured to cover all the filters and were left to dry for 24 h, covered with aluminum foil. Although this technique does not enable the chemical characterization of the stained polymers, it has proven to be an ideal protocol for the determination of MPs in environmental and biological samples, as it allows for the detection of smaller objects when combined with microscopy (e.g., ~1 µm, [59]). Particles with dimensions larger than 5 µm fall within the spatial resolution guaranteed by the FTIR microscope coupled to the FPA detector, available for this study for spectroscopic analysis (see Section 2.5). The integrated use of these two microscopic techniques has allowed us to identify and quantify natural (i.e., cellulose) and synthetic fibers and fragments with dimensions $\geq$ 0.5 µm and chemically characterize those $\geq$5 µm present in the digestive tracts of stygofauna [56].

2.4. Contamination Control

To reduce the risk of sample contamination, several precautionary measures were adopted. Yellow PP laboratory coats and blue latex gloves were used at every stage of MP processing and all treatments were performed in a clean room under a laminar flow hood [60]. In addition, the laboratory bench was regularly cleaned, and, when possible, the use of plastic equipment was avoided, using only glass or metal instead. Glassware and metal tweezers were washed and rinsed with ultrafiltered MilliQ water and then acetone (Chromasolv, Honeywell, Offenbach am Main, Germany) and left to dry under a laminar flow hood covered with aluminum foil to prevent airborne contamination. Potential sources of contamination were assessed by performing blank controls [61]. Field blanks were performed, leaving clean filters uncapped near collection points to evaluate airborne contamination during the entire sampling sessions; once in the laboratory, procedural blanks were performed by subjecting ultrafiltered MilliQ water through the sample processing steps along with environmental samples. Additionally, to evaluate atmospheric deposition, a wet filter was exposed and uncapped under the laminar flow hood during each sample processing step. All blanks were analyzed following the same methods as the samples.

2.5. Polymer Analysis

The shape, color, and size of the polymeric items on each filter were visually evaluated based on their physical characteristics through a stereomicroscope. The chemical composition of each object $\geq$ 5 µm in size was analyzed by 2D imaging Fourier Transform Infrared Spectroscopy (FTIR) using a Cary 620–670 FTIR microscope, equipped with an FPA (Focal Plane Array) 128 × 128 detector (Agilent Technologies, Santa Clara, CA, USA) and a 15× Cassegrain objective. The analysis was carried out in reflectance directly on the entire filters, using an open aperture and a spectral resolution of 8 cm^{-1}, acquiring

128 scans for each spectrum in the spectral range 3900–900 cm^{-1}. The background spectra were acquired on a golden surface. Each analysis results in a "single-tile" map with a size of 700 × 700 μm^2 (128 × 128 pixels), each pixel having a size of 5.5 × 5.5 μm^2 and providing an independent IR spectrum. Using micro-FTIR allows for combining the advantages of high spatial resolution microscopy with the chemical composition information achievable with an IR spectrometer. In each false color 2D map, the intensity of the characteristic bands of the investigated polymers was imaged. The chromatic scale of the maps shows the increasing absorbance of the bands as follows: blue < green < yellow < red. Agilent Resolution Pro software, from Agilent Technologies, was used to collect and process all spectra. Fragments and fibers were identified by comparing the obtained spectra with published spectra of plastic and cellulosic polymer standards (see Supplementary Materials, Figures S1–S9). Natural and synthetic celluloses were identified and included among the MPs because they can pose a threat to biota [47,56].

2.6. Fluorescence Microscopy

Fluorescence analysis was carried out only for fauna samples. The rationale behind this approach stems from the direct correlation between the size of MPs ingested by organisms and the size of their mouth openings. This relationship justifies the application of a technique that has a higher spatial resolution (~0.5 µm) compared to that achievable by IR spectroscopy alone (~5 µm). Since the filters required further processing to make the polymers fluorescent (see Section 2.3), this analysis was performed subsequently to the spectroscopic analysis to avoid any fluorescent interference during the collection of IR signals. Fluorescent stained filters were imaged through an epifluorescence microscope (TS2R, Nikon Europe B.V., Amstelveen, The Netherlands) equipped with a LED illuminator (pe-300 Ultra, CoolLED Ltd., Andover, UK), for which an excitation light spectrum having a maximum wavelength λ = 490 nm was selected to excite fluorescence from the stained MPs. An excitation filter with a bandpass of 455–495 nm was used to further sharpen the excitation light spectrum, and a dichroic mirror was used to direct the filtered light onto the sample. The emitted fluorescence transmitted through the dichroic mirror and filtered by an emission filter with a bandpass of 515–625 nm was collected on a Hamamatsu ORCA-Flash4.0 V3 camera. Images were acquired with a 20× magnification objective (Nikon Europe B.V., Amstelveen, The Netherlands) with N.A. = 0.75 using the HCImage software (version 4.6.0.9) provided by Hamamatsu. For each stygofauna pool, a control blank was prepared, processed, and analyzed in the same way as the sample. The particles found in the blank were subtracted from the number of particles found in the sample. Then, shape and dimension (intended as maximum length) of the fluorescent particles ≥0.5 µm were obtained by using the routine Analyze Particles of the ImageJ software [62] with the following settings: size (0.5 µm–infinity), circularity (0.00–1.00) [56].

3. Results

3.1. Groundwater Samples

MPs were detected in all groundwater samples. The abundance of MPs ranged from 18 items/L to 911 items/L, with a mean abundance of 255 items/L across the four sampling sites (Table 1). The abundance in the two karst caves, P and T_1, was significantly higher, 64 and 911 items/L, respectively, than those of the other sampling locations; namely, the groundwaters from the alluvial aquifer, T_2 and T_3 (18 and 28 items/L, respectively).

The preliminary overview through the stereomicroscope allowed for the classification of the MP particles by shape, color, and size (Table 1 and Figure 3). Colored MPs accounted for the highest proportion, followed by clear/colorless MPs, as shown in Figure 3a. The most common colors were black, red, and blue, accounting for 30, 25, and 19%, respectively. Fibers and fragments were the only two types of MPs found in the four samples (Table 1), with fibers (i.e., "long fibrous material that has a length substantially longer than its width", [63]) accounting for more than 80% in each sample, compared to the 7–12% of fragments (i.e., particles that "may have smooth or angular edges, may be flat or

angular but generally has the appearance of having broken down from a piece of larger debris", [63]). The size distribution of MP particles was classified according to four dimensional classes, from <100 µm to >1 mm (Figure 3b). The average dimension of MPs was between 100 and 500 µm, and 500 µm and 1 mm, both accounting for 34%. Only the P and T_2 groundwater samples were dominated by particles in this dimensional range, with 46% on average, while in the T_3 groundwater sample, the range 1 mm–500 µm accounted for the highest percentage, with 48%. The T_1 sample, which also showed the highest MP concentration, exhibited most of the MPs in the largest size range, >1 mm, defined as "large microplastics" [3], accounting for 62% of the abundance.

Table 1. Abundance (items/L) and percentages of the type of MPs collected from the three GWBs, P (Bossea, karst cave), T_1 (Buca del Vasaio, karst cave), T_2 (bore, alluvial aquifer), and T_3 (bore, alluvial aquifer).

Site	Abundance	Fibers	Fragments
		%	%
P	64	88	12
T_1	911	90	10
T_2	18	94	6
T_3	28	93	7

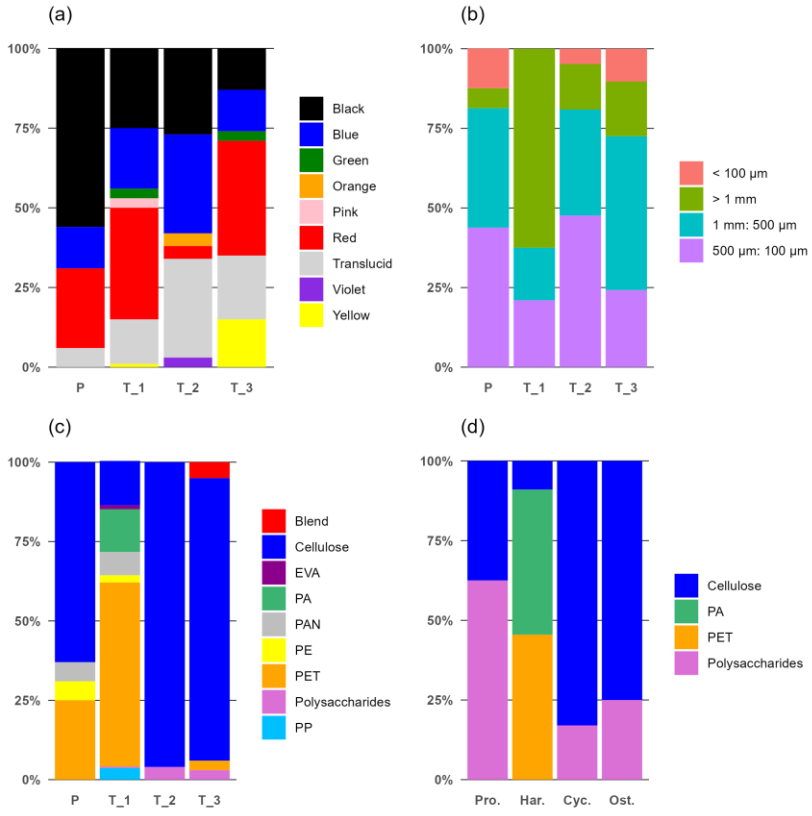

Figure 3. Percentages of (**a**) colors, (**b**) dimensional ranges, and (**c**) MP polymers ≥ 5 µm found in the water samples analyzed by microFTIR. (**d**) Percentages of MP polymers ≥ 5 µm found in the stygofauna pools from the four sampling sites analyzed by microFTIR. P: Bossea cave site, T_1: Buca del Vasaio cave, T_2: first monitoring bore, T_3: second monitoring bore. Pro.: *P. franciscoloi*; Har.: Harpacticoida, Cyc.: Cyclopoida, Ost.: Ostracoda.

2D imaging FTIR analysis allowed for identifying the nature of polymers, as shown in Figure 3c. Cellulose was found in every sample and represented the highest percentages in three sites (P, T_2, and T_3), with 82.7% on average, while for T_2, the dominant

polymer was polyethylene terephthalate, accounting for 58% of the abundance. Other polymers identified were polyamide (3.4%), polyacrylonitrile (3.4%), polyethylene (2.2%), polysaccharide gums (1.7%), PP/PE blend (1.3%), polypropylene (0.9%) and ethylene-vinyl acetate (0.3%). Infrared spectra compared to the glass fiber background filter, visible light maps, and 2D imaging false color maps of representative MPs and cellulose samples for groundwater and stygofauna pools are shown in the Supplementary files (Figures S1–S9).

3.2. Fauna Samples

Preliminary examination with visible light microscopy suggested the potential presence of MPs in the fecal pellets of certain crustacean specimens collected from the sampling sites. These specimens were not combined for subsequent MP analysis (Figure 4).

Figure 4. A female specimen of the harpacticoid *Attheyella crassa* (Sars G.O., 1863) (**left**; about 0.70 mm in length) and a detailed view of the terminal part of the digestive tract (**right**). The digestive tract contains a fecal pellet composed of fine sediment and blue particles. The specimen was collected from the T_2 site. Being an epigean species, the specimen was not pooled with the *Diacylops* individuals gathered from the bore.

The average lengths, widths, and biomass values of the four animal pools examined in this study were summarized in Table 2. The percentages of fluorescent MPs classified by shape, as well as the mean and standard deviations of length, for each taxonomic pool, are reported in Table 3. All fluorescent particles found in blank controls were counted and classified by shape, then accordingly subtracted from the relative samples.

The highest number of fluorescent particles $\geq$ 0.5 µm per biomass was detected for Harpacticoida from the T_1 site (130.5 items/µg DW), followed by those of Cyclopoida from the T_2 site (47.6 items/µg DW), Ostracoda from the T_3 site (5.3 items/µg DW), and *P. franciscoloi* from the P site (0.2 items/µg DW).

Pellets, i.e., particles that "may be spherical or granular" [63], accounted for the highest percentages for each pool, followed by fragments and fibers (Table 3 and Figure S10). In the pool of *P. franciscoloi*, pellets accounted for 93% of the abundance, while fibers and fragments accounted for 1% and 6%, respectively. In the pool of Harpacticoida, pellets accounted for 85% of the abundance, while fibers and fragments accounted for 4% and 11%,

respectively. Similarly, in the pool of Cyclopoida, pellets accounted for 75%, while fibers and fragments accounted for 4% and 21% of the abundance, respectively. Lastly, in the pool of Ostracoda, pellets accounted for 87%, while fibers and fragments accounted for 3% and 10%, respectively. Concerning dimension, fragments represented the largest fluorescent particles for each pool, with a mean size of 26 ± 30 µm, followed by fibers (19 ± 10 µm) and pellets (1 ± 1 µm).

Table 2. Mean (µ) and standard deviation (SD) of length (L; in mm), width (W; in mm), and biomass in dry weight (DW; in µg) of the individuals of the four taxonomic pools processed in this study. n indicates the number of individuals in each pool. The total biomass (TOT DW; in µg) and the number of particles per individual (items/ind) and biomass unit (items/µg) of each pool are also reported.

Taxonomic Pool	Site	µ_L (mm)	SD_L (mm)	µ_W (mm)	SD_W (mm)	µ_DW (µg)	SD_DW (µg)	TOT DW (µg)	Items/ ind.	Items/µg (TOT DW)
Proasellus franciscoloi (n = 1)	P	7.095		1.656				1,032	191	0.2
Harpacticoida (n = 15)	T_1	0.468	0.120	0.095	0.013	0.274	0.125	4	35	130.5
Cyclopoida (n = 6)	T_2	0.916	0.138	0.214	0.038	2.358	1.023	14	112	47.6
Ostracoda (n = 19)	T_3	0.562	0.070	0.334	0.046	3.160	1.251	62	17	5.3

Table 3. Classification of the fluorescent particles ≥ 0.5 µm found in stygofauna collected from the three GWBs. Percentages of pellets, fibers, and fragments (according to classification in Lusher et al. [63]) are given as follows: for each type, the mean (µ) and the standard deviation (SD) of the lengths (µm) are also reported. For pellets, the length was considered as the diameter, for fibers, as the major dimension, and for fragments, as the distance between the two most distant points.

Taxonomic Pool	Pellet			Fiber			Fragment		
	%	µ	SD	%	µ	SD	%	µ	SD
Proasellus franciscoloi (n = 1)	93	1	1	1	16	3	6	32	37
Harpacticoida (n = 15)	85	1	1	4	16	9	11	25	34
Cyclopoida (n = 6)	75	1	1	4	24	19	21	22	34
Ostracoda (n = 19)	87	2	2	3	21	10	10	23	14

As mentioned above, 2D imaging FTIR analysis was carried out for items larger than 5 µm that fell within the spatial resolution of the FPA detector. As for groundwater samples, cellulose was found in each stygofauna pool, accounting for 51% of the abundance. For the Cyclopoida and Ostracoda pool, cellulose also represented the dominant polymer, accounting for 83% and 75% of the abundances, respectively, followed by polysaccharide gums, with 17% and 25%, respectively. In the *P. franciscoloi* pool, polysaccharide gums accounted for the highest percentage (63%), followed by cellulose, with 38%. The MPs found in the Harpacticoida pool showed the highest polymeric variety, with polyethylene terephthalate and polyamide being the dominant polymers, both accounting for 45%, followed by cellulose (9%).

4. Discussion

This study provides a preliminary analysis of MP contamination in three GWBs and their resident fauna. We acknowledge the possibility that sampling in bore T_3 might have represented the MPs and fauna of the bore column rather than those of the surrounding aquifer. Unpurged wells, which draw water from shallow unconfined aquifers, constitute an artificial setting characterized by heightened levels of oxygen, organic material enrichment, potential exposure to light, and a significantly larger volume of open water when compared to the natural aquifer environment [64]. In the case of bore T_2, we are confident that this issue was less pressing since we thoroughly purged the well eight times before collecting our sample. However, we still exercised caution in our claims because the purging process itself may introduce allochthonous material to the saturated zone, which could originate from the water column of the drilling and be captured during pumping [64]. In the groundwater samples, MPs were universally present, with their abundance ranging

from 18 to 911 items/L. In particular, the Bossea cave in Piedmont (P) and the Buca del Vasaio cave in Tuscany (T_1) showed significantly higher MP concentrations compared to the alluvial aquifer bores, T_2 and T_3. Most of these MPs were colored, predominantly black, red, and blue, and consisted primarily of fibers. The average size of MPs ranged from 100 µm to 1 mm, although most MPs in the T_1 sample were >1 mm. Due to the mixed granulometric composition, caution should be exercised when attributing MPs close to 1 mm to the alluvial groundwater body. Contamination from large particles may also result from contamination of the bore water, especially in bore T_3, which was open at the top, rather than originating from the alluvial aquifer. Chemical analysis revealed cellulose as the most common polymer, with polyethylene terephthalate prevailing in certain samples. MPs were also detected in all groundwater taxa, with the highest number of MPs per biomass found in the Harpacticoida of T_1. Pellets were the most common shape of MPs in these samples, followed by fragments and fibers. The largest fluorescent particles were fragments, with an average size of 26 µm. Polymer analysis of fauna samples also identified cellulose as the predominant polymer, with variations in polymer distribution among different fauna pools.

The detection of MPs in all samples highlights a widespread contamination issue in groundwater bodies. Groundwater constitutes up to 99% of the Earth's liquid freshwater, and, in many European countries, is used mainly for drinking purposes [65]. The presence of emerging contaminants in this natural resource may threaten its quality and pose a potential health hazard [65]. The widespread presence of MPs in groundwater samples amplifies concerns about the integrity of this vital resource. Moreover, groundwater has a longer residence time than surface water, meaning that once in subsurface environments, pollutants may reside for decades [66,67].

The range of MP abundance, from 18 to 911 items per liter, is significant, even considering that, due to the lack of standardized methods for analyzing MPs in aquatic environments, comparing results with different works can be difficult. Comparing the abundances in karst cave samples with those from other karst environments highlighted that our values are significantly higher than those found in springs and shallows of karst aquifers in Illinois, USA (6.4 items/L) [17], and in a tourist karst cave in Guizhou Province, China (4.50 items/L) [54]. Bossea karst cave is comparable to that found in the spring issuing of the karst system in Missouri, USA, during flooding events (81.3 items/L) [68]. Furthermore, the MP abundance detected at this site is comparable to that shown in previous work in the Bossea cave (up to 54 items/L) [69], also suggesting that MPs from the non-touristic area can be linked to the hydrogeological connections of the underground with the shallow environment. In the second karst cave investigated, Buca del Vasaio, (T_2)—which is not a touristic cave—the number of MPs is considerably higher than in the Bossea cave (P). This may be due to the fact that touristic caves, like Bossea, impose rules of conduct for the public and are, therefore, closely monitored. The conformation of the Buca del Vasaio cave makes it accessible only to experienced speleologists, as it requires climbing with ropes and is not readily accessible otherwise, so the indirect anthropogenic impact due to human presence and the indiscriminate release of waste are not managed and can lead to a higher level of environmental pollution. The abundance of MPs found in the samples from the alluvial aquifer is comparable to that found in an Australian unconfined alluvial aquifer (average of 38.8 $\pm$ 8 items/L; [18]), but much higher than that found in the Shiraz alluvial aquifer (0.48 items/L; [66]). The number of MPs is particularly high in the two caves compared to the alluvial aquifer investigated in this study, indicating that caves are more susceptible to, or affected by, human activities leading to MP pollution. Since the underground environment is closely connected with the shallow ones, it is not difficult to hypothesize the migration of MP from the surface through porous media [17,70].

This may be relevant for karst environments, since the presence of fissures can influence the hydraulic conductivity of rock masses, thus acting as a predominant transport pathway for MPs in groundwaters [71], in addition to direct transport due to human contact with these environments.

The presence of fibers as the most common MP morphology reflects the results of other works in groundwaters, with fibers representing from 70% in the alluvial aquifer [66] to 95.1% [69], and even 100% [17] in karst environments. Synthetic clothes may be considered a major source of fiber contamination in aquatic environments [72,73], possibly arising from clothing and other textile products. The presence of fibers in groundwaters can also be attributed to their permanence in soil and subsequent remobilization due to rainfall or irrigations [17].

The colors of MPs can provide an important clue as to their origin, i.e., natural or synthetic, or the presence of other chemical contaminants [17,69]. The prevalence of colored MPs, especially black, blue, and red was found. Black and blue MPs were also prevalent in groundwaters analyzed in previous studies, e.g., [69], while a predominance of blue/clear and of black-gray and red-yellow MPs were found in others [17,66]. It has been shown how the color of MPs can influence the feeding habits of organisms, which may mistake them for trophic resources [74]. Nevertheless, in underground systems, there is no light and MP color is not significant for ingestion by the stygofauna, but in the surrounding ecosystems, epigean species may be misled by colors [69].

The size distribution of MPs, mainly between 100 and 500 µm, is in line with the size of MPs typically expected in this kind of water sample [17,18,66,69]. The presence of large microplastics (>1 mm, [3]) in the T_2 sample is significant and may be attributed to contamination from the bore water, despite purging efforts. The alternative explanation, suggesting limited weathering mechanisms in these environments, is less probable [7].

The discovery of MPs in the gut of the isopod *P. franciscoloi* and groundwater ostracods and copepods marked the first evidence of MPs in groundwater fauna. However, concerning bore T_3, and, in part, also bore T_2, it is not possible to definitively establish if the collected fauna inhabited the water column or the surrounding aquifer. The MPs' concentration varied among taxa. Ingestion of plastic debris by sediment-residing organisms is a well-documented phenomenon as well as the species–specific ingestion pattern [75]. Notably, the quantity of ingested MPs by the copepods in this study (all deposit-feeders) far exceeded 10 items per microgram of dry mass. Deposit-feeders likely ingest more particles than other feeding guilds, such as predators, as is the cyclopoid *Acanthocyclops robustus* (Sars G.O., 1863) analyzed in Di Lorenzo et al. [56]. On the other hand, estuarine copepods, such as the filter-feeder *Eurytemora affinis* (Poppe, 1880), are capable of ingesting as many as 59,000 microplastic particles per hour [76]. This suggests that the rate of MP ingestion is shaped by feeding behaviors and potentially by metabolic rates, which are typically lower in stygobitic species compared to their epigean counterparts [77]. Accordingly, the number of MPs per µg of dry weight in *P. franciscoloi* was significantly lower than in previous studies on epigean asellids (e.g., [78]). About 191 MPs, predominantly pellets, were identified in the gut of the *P. franciscoloi* specimen (adult female, approximately 5 mm in length). Given an average diameter equal to 3 µm of the MP pellets ingested by this species, the total volume of ingested MPs was estimated to be <<1% of its gut volume (1 mm^3), which was measured using RX imagery (Figure 5). This volume was significantly lower—by an order of magnitude, at least—than the 4% gut volume occupancy by MPs in an epigean Asellidae species (gut volume of 1 mm^3, as in *P. franciscoloi*) from a small lowland river in north-eastern Belgium [78]. This discrepancy is likely due to stygobitic species' lower metabolism and reduced feeding rates compared to surface-dwelling relatives [77].

It was found that groundwater taxa ingested mainly MP pellets, while fibers were the most common shape in the water samples. The predominance of pellet-shaped ingested MPs in freshwater meiofauna has already been observed in previous studies [56,75]. This result is, however, surprising because Balestra and Bellopede [79] found that fibers accounted for the majority of MPs in the Bossea cave sediments, followed by fragments and other morphologies, in line with the results observed for groundwaters at the same location [69]. However, the cut-off for MP analysis in sediment was 0.1 mm [79], while, in this study, the main focus was on smaller particles (down to 0.5 µm) that can be more easily ingested by groundwater microcrustaceans, based on the studies conducted on their

marine and freshwater relative species. For instance, the marine copepod *Acartia tonsa* Dana, 1849, demonstrates selective ingestion of plastic beads specifically within the size range of 13.9 to 59 µm [76]. In addition, biofouling phenomena increase the density of MP particles in sediments, even of small-sized beads, causing them to sink [80]. These mechanisms enhance the accessibility of nano- and microplastics to organisms living in sediment, particularly through ingestion, as the size of these particles is comparable to, or even less than, that of sediment grains (e.g., [81]). Moreover, the presence of biofilms on MPs may increase their palatability or detectability to organisms, as observed in some marine crustacean species [82,83].

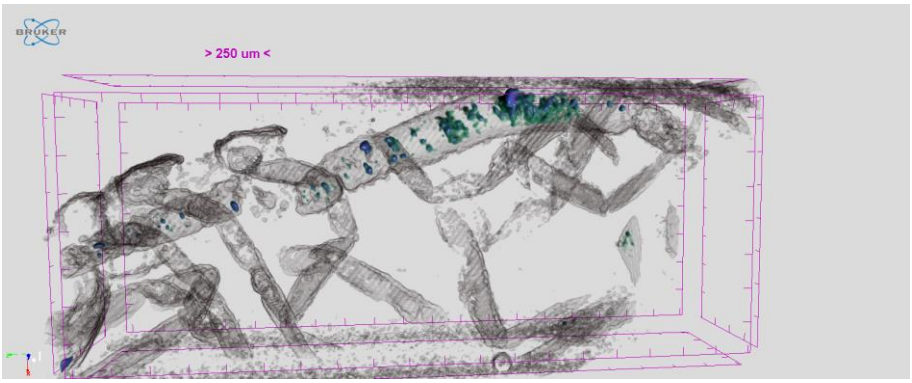

Figure 5. 3D volume reconstruction from microtomography analysis of the gut of the analyzed *P. franciscoloi*, Bossea cave. The pellets are highlighted in green/blue (see Supplementary Materials, Paragraph S11).

The polymers detected in groundwater samples were not uniformly present in biological specimens, suggesting selective ingestion of certain polymer types by the studied taxa. Additionally, some polymers might be ingested and quickly regurgitated. For instance, the estuarine copepod *Eurytemora affinis* can regurgitate latex beads [76]. However, *E. affinis* retains bacterial-coated latex microspheres, successively egested in fecal pellets [84]. This behavior highlights the selective feeding mechanisms in aquatic organisms regarding MPs. The identification of cellulose as the dominant polymer in fauna samples is a critical aspect and has already been extensively observed (e.g., [56]). The predominant polymers in groundwaters are often very diverse, such as polyethylene, polyvinyl alcohol, or polystyrene [17,66,69], but, in our results, cellulose was the most abundant polymer. This may be a hint as to their origin, considering that cellulose in surface waters is assumed to come mainly from the textile industry [47]. The presence of other polymers like polyacrylonitrile, polyethylene terephthalate, and polyamide, especially in the fauna samples, suggests a different source of MP pollution, most likely resulting from the leakage of pollution from aboveground [18].

Although it is known that the dispersed nature of possible contaminating sources and diffuse pollution pose serious challenges to managing groundwater quality [65], this study extensively explores the abundance of MPs only in groundwater and its resident fauna. Thus, further studies are needed to assess the organic contaminants leaching from MPs and their potential effects on water chemistry and groundwater obligate species [67,85]. Moreover, the long-term ecological consequences of MP ingestion on groundwater fauna are still unknown. Drawing upon findings from prior research on aquatic fauna, it is reasonable to anticipate that stygobitic species exposed to MPs may experience a spectrum of detrimental impacts (e.g., [86]) spanning from disrupted feeding patterns to compromised reproductive health. Key concerns include the likelihood of gastrointestinal damage due to the ingestion of hard MPs, shifts in energy metabolism, genetic mutations, changes in excretory functions, and complex, sometimes conflicting, interactions with other hydrophobic organic pollutants [30]. There is also a crucial need to understand how MPs transfer along food chains and the implications for higher trophic levels [87]. Groundwater fauna plays

critical roles in nutrient cycling, sediment transport, and maintaining the overall health of the ecosystem [36]. The impairment of these organisms due to MP ingestion could disrupt these vital processes, leading to broader ecological consequences.

Further aspects that would need a deeper investigation are the degradation processes and the ultimate fate of MPs in groundwater environments. Physical, chemical, and biological processes in these ecosystems can affect the degradation of MPs. Once pollution reaches the groundwater, the process is almost irreversible [65], and the persistence of pollutants in these environments can be significant, also because the dynamics of groundwater are much lower than those of surface water [88]. The potential residence time of MPs in groundwaters can be up to years [66], posing a significant ecological risk to resident fauna as well as to water quality. Finally, groundwaters often interact with surface waters [89]. The impact of MPs in groundwater could, therefore, extend to adjacent aquatic systems, spreading the ecological consequences beyond their point of origin.

A multifaceted approach is essential to manage tourist and non-tourist caves effectively and limit the occurrence of microplastics. Educating visitors about responsible plastic usage, coupled with strict waste disposal rules within cave systems, is recommended to minimize the introduction of plastics. We also recommend regular surveys and research collaborations to monitor and understand the extent of MP contamination in these habitats. Infrastructure improvements, such as designated pathways and restricted access to sensitive areas, protect cave environments. Regarding alluvial groundwater bodies beneath urban areas, managing MPs remains challenging due to diverse surface sources. Effective management requires collaboration between authorities, communities, and environmental organizations to protect urban groundwater quality.

5. Conclusions

The present study provides preliminary information on the presence of MPs in three Italian GWBs. Samples included groundwater and stygofauna pools collected from two karst caves and two monitoring bores in an alluvial aquifer. MP abundances were found to vary significantly between groundwaters, as well as between the corresponding groundwater taxa, while shape, colors, and size were comparable. Chemical characterization identified artificial/textile cellulose as the predominant polymer for each sample. The complexity of sampling biodiversity and undissolved contaminants in detrital aquifer media underscores the need for caution when interpreting findings from open wells and even purged closed boreholes.

The increasing pollution of groundwaters by MPs raises great concerns for the conservation of this sensitive environment. Besides impairing groundwater quality, which is often used for drinking purposes, it is expected to cause detrimental effects on species and communities living in this habitat. The results presented in this study provide the assumptions for further investigations to assess the potential impact of MPs and other emerging contaminants and estimate the risk assessment for human health in these environments.

Regarding the impact of MPs on groundwater fauna, it was found that each groundwater taxa ingested mainly MP pellets, while water samples mostly contained polymer fibers. Further studies are advisable to assess the role of MPs as vectors of organic contaminants through ingestion by underground fauna. The development of standardized sampling protocols for MPs is strongly encouraged, as it would enhance the comparability of results between different searches, both ecologically and environmentally. Finally, this study highlights the importance of selecting an appropriate dimensional cut-off in investigating microplastics in groundwater ecosystems. Selecting an excessively large cut-off risks underestimating the actual ingestion of these particles by groundwater species, especially if their size preferences are not comprehensively addressed.

Supplementary Materials: The following supporting information can be downloaded at: https://www.mdpi.com/article/10.3390/su16062532/s1, Figure S1: (From the left) Visible light and 2D FTIR Imaging maps of a fiber identified as textile/artificial cellulose owing to absorption 3500–3000 cm^{-1} (OH stretching), 3000–2800 cm^{-1} (CH stretching), 1727 cm^{-1} (C=O stretching), 1639 cm^{-1} (adsorbed water), 1459 and 1434 cm^{-1} (CH bending), and 1091 cm^{-1} (C-OH stretching) [90]. (Bottom) FTIR Reflectance spectra of the polymer fiber and the filter background, relating to a single pixel (5.5 × 5.5 μm^2) of the 2D imaging map. Figure S2: (From the left) Visible light and 2D FTIR Imaging maps of a fiber identified as polyamide (PA) owing to absorption 3306 cm^{-1} (Amide A), 3063 cm^{-1} (asymmetric CH stretching), 3000–2800 cm^{-1} (CH stretching), 1671 cm^{-1} (Amide I), 1565 cm^{-1} (Amide II), 1284 cm^{-1} (NH bending, C-N stretching), and 1172 cm^{-1} (CH_2 bending) [91]. (Bottom) FTIR Reflectance spectra of the polymer fiber and the filter background, relating to a single pixel (5.5 × 5.5 μm^2) of the 2D imaging map. Figure S3: (From the left) Visible light and 2D FTIR Imaging maps of a fragment identified as polyethylene (PE) owing to absorption 2950–2800 cm^{-1} (CH stretching), 1715 cm^{-1} (C=O stretching, probably due to oxidation), 1458 cm^{-1} (CH_2 bending), and 1166 cm^{-1} (wagging deformation) [91,92]. (Bottom) FTIR Reflectance spectra of the polymer fragment and the filter background, relating to a single pixel (5.5 × 5.5 μm^2) of the 2D imaging map. Figure S4: (From the left) Visible light and 2D FTIR Imaging maps of a fiber identified as polypropylene (PP) owing to absorption 3000–2800 cm^{-1} (CH stretching), 1715 cm^{-1} (C=O stretching, probably due to oxidation), 1469 cm^{-1} (CH_2 bending), 1374 cm^{-1} (CH_3 bending), 1253 cm^{-1} (CH_2 twist) and 1170 cm^{-1} (CH bending, CH_3 rocking, C-C stretching) [91,92]. (Bottom) FTIR Reflectance spectra of the polymer fiber and the filter background, relating to a single pixel (5.5 × 5.5 μm^2) of the 2D imaging map. Figure S5: (From the left) Visible light and 2D FTIR Imaging maps of a fiber identified as polyethylene terephthalate (PET) owing to absorption 3000–2950 cm^{-1} (CH stretching), 1724 cm^{-1} (C=O stretching), 1571 and 1502 cm^{-1} (vibrations aromatic skeleton with stretching C=C), 1412 cm^{-1} (stretching of the C-O group deformation of the O-H group, and bending and wagging vibrational modes of the ethylene glycol segment), 1297 and 1141 cm^{-1} (terephthalate Group $OOCC_6H_4$-COO) [91]. (Bottom) FTIR Reflectance spectra of the polymer fiber and the filter background, relating to a single pixel (5.5 × 5.5 μm^2) of the 2D imaging map. Figure S6: (From the left) Visible light and 2D FTIR Imaging maps of a fiber identified as a polymeric blend of polypropylene and polyethylene (PE/PP) owing to absorption 3000–2800 cm^{-1} (CH stretching), 1791 cm^{-1} (C=O stretching probably due to oxidation), 1460 cm^{-1} (CH_2 bending), and 1376 cm^{-1} (CH_3 bending) [91]. (Bottom) FTIR Reflectance spectra of the polymer fiber and the filter background, relating to a single pixel (5.5 × 5.5 μm^2) of the 2D imaging map. Figure S7: (From the left) Visible light and 2D FTIR Imaging maps of a fragment identified as ethylene-vinyl acetate (EVA) owing to absorption ~3300 cm^{-1} (OH stretching), 3000–2850 cm^{-1} (CH stretching), 1739 cm^{-1} (C=O stretching), 1481 cm^{-1} (CH_2 and CH_3 bending), 1389 cm^{-1} (CH_3 bending), 1281 cm^{-1} (C(=O)O stretching) [91]. (Bottom) FTIR Reflectance spectra of the polymer fragment and the filter background, relating to a single pixel (5.5 × 5.5 μm^2) of the 2D imaging map. Figure S8: (From the left) Visible light and 2D FTIR Imaging maps of a fragment identified as polysaccharide gum owing to absorption ~3500 cm^{-1} (OH stretching), 3000–2800 cm^{-1} (C=O stretching), 1674 and 1580 cm^{-1} (C=C stretching), and 1382 cm^{-1} (CH bending) [93,94]. Although the similarity with the cellulose spectrum, the shape of the item and the presence of several functional groups allowed the above-mentioned polymeric assignment. (Bottom) FTIR Reflectance spectra of the polymer fragment and the filter background, relating to a single pixel (5.5 × 5.5 μm^2) of the 2D imaging map. Figure S9: (From the left) Visible light and 2D FTIR Imaging maps of a fiber identified as polyacrylonitrile (PAN) owing to absorption 2930 and 2872 cm^{-1} (=C-H stretching), 2240 cm^{-1} (CN stretching), 1731 cm^{-1} (C=O stretching probably due to oxidation), 1455 and 1361 cm^{-1} (CH_2 bending), and 1068 cm^{-1} (CH stretching) [91,95]. (Bottom) FTIR Reflectance spectra of the polymer fiber and the filter background, relating to a single pixel (5.5 × 5.5 μm^2) of the 2D imaging map. Figure S10: Example of (a) polymer pellets from the Harpacticoida pool and (b) polymer fragment and pellet from the Ostracoda pool visualized at the epifluorescence microscope (ex: 455–495 nm; em. 515–625 nm). Paragraph S11: Micro-computed tomography (μ-CT).

Author Contributions: Conceptualization, L.S., T.D.L., T.M., A.C. and D.M.P.G.; Data curation, L.S., D.C., S.B.C., L.P., A.T.D.C., T.D.L. and M.L.; Formal analysis, L.S., A.T.D.C., D.C., S.C. and S.B.C.; Funding acquisition, A.C. and T.D.L.; Investigation, L.S., T.D.L., A.T.D.C. and S.B.C.; Methodology, L.S., T.D.L., T.M., D.C., M.L. and S.C.; Project administration, A.C. and T.D.L.; Resources, T.D.L. and A.C.; Sample collection: L.S., L.P., V.B., T.D.L. and A.T.D.C.; Software, L.S. and A.T.D.C.; Supervision, A.C., T.D.L., T.M. and D.M.P.G.; Validation, A.C., T.D.L., D.M.P.G., V.B., L.P. and T.M.; Visualization: L.S., A.T.D.C., S.C. and D.C.; Writing—original draft, L.S., A.T.D.C., T.D.L., V.B., S.C., L.P. and M.L.; Writing—review and editing, all. All authors have read and agreed to the published version of the manuscript.

Funding: A.C. and L.S. acknowledge funding from the European Union—Next Generation EU. National Recovery and Resilience Plan (NRRP)—M4C2 Investment 1.3—Research Programme PE_00000005 "RETURN"—CUP B83C22004820002. Views and opinions expressed are however those of the author(s) only and do not necessarily reflect those of the European Union or the European Commission. Neither the European Union nor the European Commission can be held responsible for them. T.D.L. and D.M.P.G. acknowledge funding from Biodiversa+ DarCo, the European Biodiversity Partnership under the 2021-2022 BiodivProtect joint call for research proposals, co-funded by the European Commission (GA N°101052342) and with the funding organizations Ministry of Universities and Research (Italy), Agencia Estatal de Investigación—Fundación Biodiversidad (Spain), Fundo Regional para a Ciência e Tecnologia (Portugal), Suomen Akatemia—Ministry of the Environment (Finland), Belgian Science Policy Office (Belgium), Agence Nationale de la Recherche (France), Deutsche Forschungsgemeinschaft e.V. (Germany), Schweizerischer Nationalfonds (Grant N° 31BD30_209583, Switzerland), Fonds zur Förderung der Wissenschaftlichen Forschung (Austria), Ministry of Higher Education, Science and Innovation (Slovenia), and the Executive Agency for Higher Education, Research, Development and Innovation Funding (Romania). T.D.L. also acknowledges funds from the European Union—NextGenerationEU, Italian Ministry of University and Research, P.N.R.R., Missione 4 Componente 2, "Dalla ricerca all'impresa", Investimento 1.4, Project CN00000033 and LIFE financial instrument of the European Union (LIFE19 ENV/FR/000086) in the framework of the AIRFRESH project "Air pollution removal by urban forests for a better human well-being".

Institutional Review Board Statement: Not applicable.

Informed Consent Statement: Not applicable.

Data Availability Statement: Data are contained within the article or Supplementary Materials.

Acknowledgments: We thank Jacopo Manzini and Moreno Lazzara (CNR-IRET) for their support in the sampling surveys.

Conflicts of Interest: The authors declare no conflicts of interest.

References

1. PlasticsEurope; EPRO. *Plastics—The Facts 2021 an Analysis of European Plastics Production, Demand and Waste Data*; PlasticsEurope: Brussels, Belgium; EPRO: Wemmel, Belgium, 2021.
2. Taylor, M.L.; Gwinnett, C.; Robinson, L.F.; Woodall, L.C. Plastic microfibre ingestion by deep-sea organisms. *Sci. Rep.* **2016**, *6*, 33997. [CrossRef]
3. *ISO/TR 21960:2020(en)*; Plastics—Environmental Aspects—State of Knowledge and Methodologies. 2020. Available online: https://www.iso.org/obp/ui/en/#iso:std:iso:tr:21960:ed-1:v1:en (accessed on 9 October 2023).
4. Guerranti, C.; Martellini, T.; Perra, G.; Scopetani, C.; Cincinelli, A. Microplastics in cosmetics: Environmental issues and needs for global bans. *Environ. Toxicol. Pharmacol.* **2019**, *68*, 75–79. [CrossRef]
5. UNEP. *Plastic in Cosmetics: Are We Polluting the Environment through Our Personal Care?* UNEP: Nairobi, Kenya, 2015.
6. Cole, M.; Lindeque, P.; Halsband, C.; Galloway, T.S. Microplastics as contaminants in the marine environment: A review. *Mar. Pollut. Bull.* **2011**, *62*, 2588–2597. [CrossRef] [PubMed]
7. Crawford, C.B.; Quinn, B. *Microplastic Pollutants*, 1st ed.; Elsevier Science: Amsterdam, The Netherlands, 2016; pp. 1–315.
8. Zhang, K.; Hamidian, A.H.; Tubić, A.; Zhang, Y.; Fang, J.K.; Wu, C.; Lam, P.K. Understanding plastic degradation and microplastic formation in the environment: A review. *Environ. Pollut.* **2021**, *274*, 116554. [CrossRef] [PubMed]
9. Allen, S.; Allen, D.; Phoenix, V.R.; Le Roux, G.; Jiménez, P.D.; Simonneau, A.; Binet, S.; Galop, D. Atmospheric transport and deposition of microplastics in a remote mountain catchment. *Nat. Geosci.* **2019**, *12*, 339–344. [CrossRef]
10. Sarma, H.; Hazarika, R.P.; Kumar, V.; Roy, A.; Pandit, S.; Prasad, R. Microplastics in marine and aquatic habitats: Sources, impact, and sustainable remediation approaches. *Environ. Sustain.* **2022**, *5*, 39–49. [CrossRef]

11. Scopetani, C.; Chelazzi, D.; Cincinelli, A.; Martellini, T.; Leiniö, V.; Pellinen, J. Hazardous contaminants in plastics contained in compost and agricultural soil. *Chemosphere* **2022**, *293*, 133645. [CrossRef]
12. Yang, H.; Chen, G.; Wang, J. Microplastics in the marine environment: Sources, fates, impacts and microbial degradation. *Toxics* **2021**, *9*, 41. [CrossRef]
13. Cincinelli, A.; Scopetani, C.; Chelazzi, D.; Martellini, T.; Pogojeva, M.; Slobodnik, J. Microplastics in the Black Sea sediments. *Sci. Total. Environ.* **2020**, *760*, 143898. [CrossRef] [PubMed]
14. Giarrizzo, T.; Andrade, M.C.; Schmid, K.; O Winemiller, K.; Ferreira, M.; Pegado, T.; Chelazzi, D.; Cincinelli, A.; Fearnside, P.M. Amazonia: The new frontier for plastic pollution. *Front. Ecol. Environ.* **2019**, *17*, 309–310. [CrossRef]
15. Van Cauwenberghe, L.; Vanreusel, A.; Mees, J.; Janssen, C.R. Microplastic pollution in deep-sea sediments. *Environ. Pollut.* **2013**, *182*, 495–499. [CrossRef] [PubMed]
16. Mintenig, S.M.; Löder, M.G.J.; Primpke, S.; Gerdts, G. Low numbers of microplastics detected in drinking water from ground water sources. *Sci. Total. Environ.* **2019**, *648*, 631–635. [CrossRef] [PubMed]
17. Panno, S.V.; Kelly, W.R.; Scott, J.; Zheng, W.; McNeish, R.E.; Holm, N.; Hoellein, T.J.; Baranski, E.L. Microplastic Contamination in Karst Groundwater Systems. *Groundwater* **2019**, *57*, 189–196. [CrossRef] [PubMed]
18. Samandra, S.; Johnston, J.M.; Jaeger, J.E.; Symons, B.; Xie, S.; Currell, M.; Ellis, A.V.; Clarke, B.O. Microplastic contamination of an unconfined groundwater aquifer in Victoria, Australia. *Sci. Total. Environ.* **2022**, *802*, 149727. [CrossRef] [PubMed]
19. Re, V. Shedding light on the invisible: Addressing the potential for groundwater contamination by plastic microfibers. *Hydrogeol. J.* **2019**, *27*, 2719–2727. [CrossRef]
20. Belkhiri, A.H.; Carre, F.; Quiot, F. State of knowledge and future research needs on microplastics in groundwater. *J. Water Health* **2022**, *20*, 1479–1496. [CrossRef]
21. Severini, E.; Ducci, L.; Sutti, A.; Robottom, S.; Sutti, S.; Celico, F. River–Groundwater Interaction and Recharge Effects on Microplastics Contamination of Groundwater in Confined Alluvial Aquifers. *Water* **2022**, *14*, 1913. [CrossRef]
22. Jiang, S.; Wang, J.; Wu, F.; Xu, S.; Liu, J.; Chen, J. Extensive abundances and characteristics of microplastic pollution in the karst hyporheic zones of urban rivers. *Sci. Total. Environ.* **2023**, *857*, 159616. [CrossRef]
23. Bergami, E.; Manno, C.; Cappello, S.; Vannuccini, M.; Corsi, I. Nanoplastics affect moulting and faecal pellet sinking in Antarctic krill (*Euphausia superba*) juveniles. *Environ. Int.* **2020**, *143*, 105999. [CrossRef]
24. Expósito, N.; Rovira, J.; Sierra, J.; Gimenez, G.; Domingo, J.L.; Schuhmacher, M. Levels of microplastics and their characteristics in molluscs from North-West Mediterranean Sea: Human intake. *Mar. Pollut. Bull.* **2002**, *181*, 113843. [CrossRef]
25. Hirai, H.; Takada, H.; Ogata, Y.; Yamashita, R.; Mizukawa, K.; Saha, M.; Kwan, C.; Moore, C.; Gray, H.; Laursen, D.; et al. Organic micropollutants in marine plastics debris from the open ocean and remote and urban beaches. *Mar. Pollut. Bull.* **2011**, *62*, 1683–1692. [CrossRef] [PubMed]
26. Cheng, Z.; Lin, X.; Wu, M.; Lu, G.; Hao, Y.; Mo, C.; Li, Q.; Wu, J.; Wu, J.; Hu, B.X. Combined Effects of Polyamide Microplastics and Hydrochemical Factors on the Transport of Bisphenol A in Groundwater. *Separations* **2023**, *10*, 123. [CrossRef]
27. Perestrelo, R.; Silva, C.L.; Algarra, M.; Câmara, J.S. Evaluation of the Occurrence of Phthalates in Plastic Materials Used in Food Packaging. *Appl. Sci.* **2021**, *11*, 2130. [CrossRef]
28. Selvam, S.; Jesuraja, K.; Venkatramanan, S.; Roy, P.D.; Kumari, V.J. Hazardous microplastic characteristics and its role as a vector of heavy metal in groundwater and surface water of coastal south India. *J. Hazard. Mater.* **2021**, *402*, 123786. [CrossRef] [PubMed]
29. Li, J.; Zhang, K.; Zhang, H. Adsorption of antibiotics on microplastics. *Environ. Pollut.* **2018**, *237*, 460–467. [CrossRef]
30. Anbumani, S.; Kakkar, P. Ecotoxicological effects of microplastics on biota: A review. *Environ. Sci. Pollut. Res.* **2018**, *25*, 14373–14396. [CrossRef]
31. Hahladakis, J.N.; Velis, C.A.; Weber, R.; Iacovidou, E.; Purnell, P. An overview of chemical additives present in plastics: Migration, release, fate and environmental impact during their use, disposal and recycling. *J. Hazard. Mater.* **2018**, *344*, 179–199. [CrossRef]
32. Malard, F.; Griebler, C.; Rétaux, S. *Groundwater Ecology and Evolution*, 2nd ed.; Academic Press: Cambridge, MA, USA, 2023; pp. 1–610. [CrossRef]
33. Rétaux, S.; Jeffery, W.R. Voices from the underground: Animal models for the study of trait evolution during groundwater colonization and adaptation. In *Groundwater Ecology and Evolution*, 2nd ed.; Malard, F., Griebler, C., Rétaux, S., Eds.; Academic Press: Cambridge, MA, USA, 2023; Chapter 12, pp. 285–304. [CrossRef]
34. Cooper, S.; Fišer, C.; Zakšek, V.; Delić, T.; Borko, Š.; Faille, A.; Humphreys, W. Phylogenies reveal speciation dynamics: Case studies from groundwater. In *Groundwater Ecology and Evolution*, 2nd ed.; Malard, F., Griebler, C., Rétaux, S., Eds.; Academic Press: Cambridge, MA, USA, 2023; Chapter 7, pp. 165–183. [CrossRef]
35. Zagmajster, M.; Ferreira, R.L.; Humphreys, W.F.; Niemiller, M.L.; Malard, F. Patterns and determinants of richness and composition of the groundwater fauna. In *Groundwater Ecology and Evolution*, 2nd ed.; Malard, F., Griebler, C., Rétaux, S., Eds.; Academic Press: Cambridge, MA, USA, 2023; Chapter 6, pp. 141–164. [CrossRef]
36. Mermillod-Blondin, F.; Hose, G.C.; Simon, K.S.; Korbel, K.; Avramov, M.; Vorste, R. Vander. Role of invertebrates in groundwater ecosystem processes and services. In *Groundwater Ecology and Evolution*, 2nd ed.; Malard, F., Griebler, C., Rétaux, S., Eds.; Academic Press: Cambridge, MA, USA, 2023; Chapter 11, pp. 263–281. [CrossRef]
37. Deng, L.; Krauss, S.; Feichtmayer, J.; Hofmann, R.; Arndt, H.; Griebler, C. Grazing of heterotrophic flagellates on viruses is driven by feeding behaviour. *Environ. Microbiol. Rep.* **2014**, *6*, 325–330. [CrossRef]

38. de Sá, L.C.; Luís, L.G.; Guilhermino, L. Effects of microplastics on juveniles of the common goby (*Pomatoschistus microps*): Confusion with prey, reduction of the predatory performance and efficiency, and possible influence of developmental conditions. *Environ. Pollut.* **2015**, *196*, 359–362. [CrossRef]
39. Jeong, C.-B.; Won, E.-J.; Kang, H.-M.; Lee, M.-C.; Hwang, D.-S.; Hwang, U.-K.; Zhou, B.; Souissi, S.; Lee, S.-J.; Lee, J.-S. Microplastic Size-Dependent Toxicity, Oxidative Stress Induction, and p-JNK and p-p38 Activation in the Monogonont Rotifer (*Brachionus koreanus*). *Environ. Sci. Technol.* **2016**, *50*, 8849–8857. [CrossRef]
40. Banzato, C.; Dallagiovanna, G.; Maino, M.; Peano, G.; Vigna, B. Correlation between the geological setting and groundwater flow: The Bossea karst underground laboratory. *Epitome* **2011**, *4*, 14.
41. Peano, G.; Vigna, B.; Villavecchia, E. L'evento alluvionale nell'ottobre 1996 nella Grotta di Bossea. *Bossea* **2005**, *5–8*, 407–422.
42. Forti, P.; Gamberi, M.L. Le pisoliti della Buca del Vasaio di Montrone e l'ipotesi del minimo e massimo diametro possibile. *Sotterranea* **1982**, *59*, 18–23.
43. Regione Toscana. Delibera n. 939 del 26/10/2009. Individuazione e Caratterizzazione dei Corpi Idrici Della Toscana—Attuazione delle Disposizioni di Cui ALL'ART.2 del DM 131/08 (Acque Superficiali) e Degli Art. 1,3 e all. 1 del D.Lgs. 30/09 (Acque Sotterranee). 2009. Available online: https://www.arpat.toscana.it/documentazione/normativa/normativa-regionale-toscana/2009/delibera-giunta-regionale-toscana-n.-939-del-26-10-2009 (accessed on 5 January 2024).
44. Bencini, A.; Ercolanelli, R.; Sbaragli, A.; Verrucchi, C. Groundwaters of Florence (Italy): Trace element distribution and vulnerability of the aquifers. *Environl. Geol.* **1993**, *22*, 193–200. [CrossRef]
45. Koelmans, A.A.; Nor, N.H.M.; Hermsen, E.; Kooi, M.; Mintenig, S.M.; De France, J. Microplastics in freshwaters and drinking water: Critical review and assessment of data quality. *Water Res.* **2019**, *155*, 410–422. [CrossRef]
46. Dris, R.; Imhof, H.; Sanchez, W.; Gasperi, J.; Galgani, F.; Tassin, B.; Laforsch, C. Beyond the ocean: Contamination of freshwater ecosystems with (micro-)plastic particles. *Environ. Chem.* **2015**, *12*, 539–550. [CrossRef]
47. Santini, S.; De Beni, E.; Martellini, T.; Sarti, C.; Randazzo, D.; Ciraolo, R.; Scopetani, C.; Cincinelli, A. Occurrence of Natural and Synthetic Micro-Fibers in the Mediterranean Sea: A Review. *Toxics* **2022**, *10*, 391. [CrossRef]
48. Castaño-Sánchez, A.; Malard, F.; Kalčíková, G.; Reboleira, A.S.P.S. Novel Protocol for Acute In Situ Ecotoxicity Test Using Native Crustaceans Applied to Groundwater Ecosystems. *Water* **2021**, *13*, 1132. [CrossRef]
49. Malard, F.; Bernard, C.; Lyon, U.; Claude, M.-J.D.-O.; Lyon, B.U.; Stoch, F. Sampling Manual for the Assessment of Regional Groundwater Biodiversity. 2002. Available online: https://www.researchgate.net/publication/267567541 (accessed on 12 January 2024).
50. Korbel, K.; Chariton, A.; Stephenson, S.; Greenfield, P.; Hose, G.C. Wells provide a distorted view of life in the aquifer: Implications for sampling, monitoring and assessment of groundwater ecosystems. *Sci. Rep.* **2017**, *7*, 40702. [CrossRef]
51. Reiss, J.; Schmid-Araya, J.M. Existing in plenty: Abundance, biomass and diversity of ciliates and meiofauna in small streams. *Freshw. Biol.* **2008**, *53*, 652–668. [CrossRef]
52. Cummins, K.W.; Wilzbach, M.; Kolouch, B.; Merritt, R. Estimating Macroinvertebrate Biomass for Stream Ecosystem Assessments. *Int. J. Environ. Res. Public Health* **2022**, *19*, 3240. [CrossRef]
53. Culver, D.C.; Pipan, T.; Fišer, Ž. Ecological and evolutionary jargon in subterranean biology. In *Groundwater Ecology and Evolution*, 2nd ed.; Malard, F., Griebler, C., Rétaux, S., Eds.; Academic Press: Cambridge, MA, USA, 2023; Chapter 4, pp. 89–100. [CrossRef]
54. Venarsky, M.; Niemiller, M.L.; Fišer, C.; Saclier, N.; Moldovan, O.T. Life histories in groundwater organisms. In *Groundwater Ecology and Evolution*, 2nd ed.; Malard, F., Griebler, C., Rétaux, S., Eds.; Academic Press: Cambridge, MA, USA, 2023; Chapter 19, pp. 439–456. [CrossRef]
55. An, X.; Li, W.; Lan, J.; Adnan, M. Preliminary Study on the Distribution, Source, and Ecological Risk of Typical Microplastics in Karst Groundwater in Guizhou Province, China. *Int. J. Environ. Res. Public Health* **2022**, *19*, 14751. [CrossRef]
56. Cutroneo, L.; Reboa, A.; Geneselli, I.; Capello, M. Considerations on salts used for density separation in the extraction of microplastics from sediments. *Mar. Pollut. Bull.* **2021**, *166*, 112216. [CrossRef]
57. Di Lorenzo, T.; Cabigliera, S.B.; Martellini, T.; Laurati, M.; Chelazzi, D.; Galassi, D.M.P.; Cincinelli, A. Ingestion of microplastics and textile cellulose particles by some meiofaunal taxa of an urban stream. *Chemosphere* **2023**, *310*, 136830. [CrossRef]
58. *ISO 6330:2021*; Textiles—Domestic Washing and Drying Procedures for Textile Testing. 2021. Available online: https://www.iso.org/standard/75934.html (accessed on 20 February 2024).
59. Alfonso, M.B.; Takashima, K.; Yamaguchi, S.; Tanaka, M.; Isobe, A. Microplastics on plankton samples: Multiple digestion techniques assessment based on weight, size, and FTIR spectroscopy analyses. *Mar. Pollut. Bull.* **2021**, *173*, 113027. [CrossRef]
60. Prata, J.C.; Sequeira, I.F.; Monteiro, S.S.; Silva, A.L.P.; da Costa, J.P.; Dias-Pereira, P.; Fernandes, A.J.S.; da Costa, F.M.; Duarte, A.C.; Rocha-Santos, T. Preparation of biological samples for microplastic identification by Nile Red. *Sci. Total. Environ.* **2021**, *783*, 147065. [CrossRef]
61. Scopetani, C.; Esterhuizen-Londt, M.; Chelazzi, D.; Cincinelli, A.; Setälä, H.; Pflugmacher, S. Self-contamination from clothing in microplastics research. *Ecotoxicol. Environ. Saf.* **2020**, *189*, 110036. [CrossRef] [PubMed]
62. Brander, S.M.; Renick, V.C.; Foley, M.M.; Steele, C.; Woo, M.; Lusher, A.; Carr, S.; Helm, P.; Box, C.; Cherniak, S.; et al. Sampling and Quality Assurance and Quality Control: A Guide for Scientists Investigating the Occurrence of Microplastics Across Matrices. *Appl. Spectrosc.* **2020**, *74*, 1099–1125. [CrossRef]
63. Schneider, C.A.; Rasband, W.S.; Eliceiri, K.W. NIH Image to ImageJ: 25 Years of image analysis. *Nat. Methods* **2012**, *9*, 671–675. [CrossRef] [PubMed]

64. Lusher, A.L.; Bråte, I.L.N.; Munno, K.; Hurley, R.R.; Welden, N.A. Is It or Isn't It: The Importance of Visual Classification in Microplastic Characterization. *Appl. Spectrosc.* **2020**, *74*, 1139–1153. [CrossRef] [PubMed]
65. UNESCO. Groundwater: Making the invisible visible. The United Nations World Water Development Report 2022. 2022. Available online: https://www.unwater.org/publications/un-world-water-development-report-2022 (accessed on 18 December 2023).
66. Esfandiari, A.; Abbasi, S.; Peely, A.B.; Mowla, D.; Ghanbarian, M.A.; Oleszczuk, P.; Turner, A. Distribution and transport of microplastics in groundwater (Shiraz aquifer, southwest Iran). *Water Res.* **2022**, *220*, 118622. [CrossRef]
67. Lapworth, D.J.; Baran, N.; Stuart, M.E.; Ward, R.S. Emerging organic contaminants in groundwater: A review of sources, fate and occurrence. *Environ. Pollut.* **2012**, *163*, 287–303. [CrossRef] [PubMed]
68. Baraza, T.; Hasenmueller, E.A. Floods enhance the abundance and diversity of anthropogenic microparticles (including microplastics and treated cellulose) transported through karst systems. *Water Res.* **2023**, *242*, 120204. [CrossRef]
69. Balestra, V.; Vigna, B.; De Costanzo, S.; Bellopede, R. Preliminary investigations of microplastic pollution in karst systems, from surface watercourses to cave waters. *J. Contam. Hydrol.* **2023**, *252*, 104117. [CrossRef] [PubMed]
70. Ren, Z.; Gui, X.; Xu, X.; Zhao, L.; Qiu, H.; Cao, X. Microplastics in the soil-groundwater environment: Aging, migration, and co-transport of contaminants—A critical review. *J. Hazard. Mater.* **2021**, *419*, 126455. [CrossRef]
71. Viaroli, S.; Lancia, M.; Re, V. Microplastics contamination of groundwater: Current evidence and future perspectives. A review. *Sci. Total. Environ.* **2022**, *824*, 153851. [CrossRef]
72. Browne, M.A.; Crump, P.; Niven, S.J.; Teuten, E.; Tonkin, A.; Galloway, T.; Thompson, R. Accumulation of microplastic on shorelines worldwide: Sources and sinks. *Environ. Sci. Technol.* **2011**, *45*, 9175–9179. [CrossRef]
73. De Falco, F.; Cocca, M.; Avella, M.; Thompson, R.C. Microfiber Release to Water, Via Laundering, and to Air, via Everyday Use: A Comparison between Polyester Clothing with Differing Textile Parameters. *Environ. Sci. Technol.* **2020**, *54*, 3288–3296. [CrossRef]
74. Schuyler, Q.; Hardesty, B.D.; Wilcox, C.; Townsend, K. To Eat or not to eat? debris selectivity by marine turtles. *PLoS ONE* **2012**, *7*, e40884. [CrossRef]
75. Scherer, C.; Brennholt, N.; Reifferscheid, G.; Wagner, M. Feeding type and development drive the ingestion of microplastics by freshwater invertebrates. *Sci. Rep.* **2017**, *7*, 17006. [CrossRef]
76. Wright, S.L.; Thompson, R.C.; Galloway, T.S. The physical impacts of microplastics on marine organisms: A review. *Environ. Pollut.* **2013**, *178*, 483–492. [CrossRef]
77. Di Lorenzo, T.; Reboleira, A.S.P.S.; Galassi, D.M.P.; Hervant, F.; Avramov, M.; Iepure, S.G.; Mammola, S. Physiological tolerance and ecotoxicological constraints of groundwater fauna. In *Groundwater Ecology and Evolution*, 2nd ed.; Malard, F., Griebler, C., Rétaux, S., Eds.; Academic Press: Cambridge, MA, USA, 2023; Chapter 20, pp. 457–479. [CrossRef]
78. Pan, C.-G.; Mintenig, S.M.; Redondo-Hasselerharm, P.E.; Neijenhuis, P.H.M.W.; Yu, K.-F.; Wang, Y.-H.; Koelmans, A.A. Automated µFTIR Imaging Demonstrates Taxon-Specific and Selective Uptake of Microplastic by Freshwater Invertebrates. *Environ. Sci. Technol.* **2021**, *55*, 9916–9925. [CrossRef] [PubMed]
79. Balestra, V.; Bellopede, R. Microplastic pollution in show cave sediments: First evidence and detection technique. *Environ. Pollut.* **2022**, *292*, 118261. [CrossRef]
80. Liu, S.; Huang, Y.; Luo, D.; Wang, X.; Wang, Z.; Ji, X.; Chen, Z.; Dahlgren, R.A.; Zhang, M.; Shang, X. Integrated effects of polymer type, size and shape on the sinking dynamics of biofouled microplastics. *Water Res.* **2022**, *220*, 118656. [CrossRef]
81. Haegerbaeumer, A.; Mueller, M.-T.; Fueser, H.; Traunspurger, W. Impacts of micro- and nano-sized plastic particles on benthic invertebrates: A literature review and gap analysis. *Front. Environ. Sci.* **2019**, *7*, 425457. [CrossRef]
82. Vroom, R.J.; Koelmans, A.A.; Besseling, E.; Halsband, C. Aging of microplastics promotes their ingestion by marine zooplankton. *Environ. Pollut.* **2017**, *231*, 987–996. [CrossRef] [PubMed]
83. Hodgson, D.; Bréchon, A.; Thompson, R. Ingestion and fragmentation of plastic carrier bags by the amphipod Orchestia gammarellus: Effects of plastic type and fouling load. *Mar. Pollut. Bull.* **2018**, *127*, 154–159. [CrossRef]
84. Powell, M.D.; Berry, A. Ingestion and regurgitation of living and inert materials by the estuarine copepod Eurytemora affinis (Poppe) and the influence of salinity. *Estuar. Coast. Shelf Sci.* **1990**, *31*, 763–773. [CrossRef]
85. Xu, B.; Liu, S.; Zhou, J.L.; Zheng, C.; Weifeng, J.; Chen, B.; Zhang, T.; Qiu, W. PFAS and their substitutes in groundwater: Occurrence, transformation and remediation. *J. Hazard. Mater.* **2021**, *412*, 125159. [CrossRef]
86. Zhang, S.; Wu, H.; Hou, J. Progress on the Effects of Microplastics on Aquatic Crustaceans: A Review. *Int. J. Mol. Sci.* **2023**, *24*, 5523. [CrossRef]
87. Batel, A.; Linti, F.; Scherer, M.; Erdinger, L.; Braunbeck, T. Transfer of benzo[*a*]pyrene from microplastics to *Artemia* nauplii and further to zebrafish via a trophic food web experiment: CYP1A induction and visual tracking of persistent organic pollutants. *Environ. Toxicol. Chem.* **2016**, *35*, 1656–1666. [CrossRef]
88. Beckie, R.D. Groundwater. In *Reference Module in Earth Systems and Environmental Sciences*; Elsevier: Amsterdam, The Netherlands, 2013. [CrossRef]
89. Saccò, M.; Mammola, S.; Altermatt, F.; Alther, R.; Bolpagni, R.; Brancelj, A.; Brankovits, D.; Fišer, C.; Gerovasileiou, V.; Griebler, C.; et al. Groundwater is a hidden global keystone ecosystem. *Glob. Chang. Biol.* **2024**, *30*, e17066. [CrossRef]
90. Garside, P.; Wyeth, P. Identification of Cellulosic Fibres by FTIR Spectroscopy: Thread and Single Fibre Analysis. *Stud. Conserv.* **2003**, *48*, 269–275. [CrossRef]

91. Jung, M.R.; Horgen, F.D.; Orski, S.V.; Rodriguez, C.V.; Beers, K.L.; Balazs, G.H.; Jones, T.T.; Work, T.M.; Brignac, K.C.; Royer, S.J.; et al. Validation of ATR FT-IR to identify polymers of plastic marine debris, including those ingested by marine organisms. *Mar. Pollut. Bull.* **2018**, *127*, 704–716. [CrossRef] [PubMed]
92. Wang, C.; Wang, Y.; Dang, Y.; Jiao, Q.; Li, H.; Wu, Q.; Zhao, Y. Synthesis of a novel titanium complex catalyst and its catalytic performance for olefin polymerization. *Russ. J. Appl. Chem.* **2015**, *88*, 1723–1727. [CrossRef]
93. Faria, S.; Petkowicz, C.L.D.O.; de Morais, S.A.L.; Terrones, M.G.H.; de Resende, M.M.; de França, F.P.; Cardoso, V.L. Characterization of xanthan gum produced from sugar cane broth. *Carbohydr. Polym.* **2011**, *86*, 469–476. [CrossRef]
94. Hong, T.; Yin, J.-Y.; Nie, S.-P.; Xie, M.-Y. Applications of infrared spectroscopy in polysaccharide structural analysis: Progress, challenge and perspective. *Food Chem.* **2012**, *12*, 100168. [CrossRef] [PubMed]
95. Mizher, R.M.; Adawiya J, H.; Naser, J.Z.; Wee, T.T.; Zaki B, A.R.M.; Bin, K.A. Synthesis and characterization of grafted Acrylonitrile on Polystyrene modified with carbon nanotubes using Gamma-irradiation. *Res. J. Chem. Sci.* **2012**, *2*, 790–795. [CrossRef]